FIBRE REINFORCED SOILS FOR GEOTECHNICAL INFRASTRUCTURE

Adrian R. Russell[1], Andrea Diambra[2], Erdin Ibraim[2] and David Muir Wood[2]
[1] *Centre for Infrastructure Engineering and Safety, School of Civil and Environmental Engineering, University of New South Wales, Sydney, Australia*
[2] *Department of Civil Engineering, University of Bristol, Bristol, United Kingdom*

ABSTRACT

This paper presents the results of recent laboratory studies on fibre reinforced soils. Drained and undrained triaxial test results highlight how soil stress-strain behaviour may be altered by mixing with discrete flexible fibres. In triaxial compression a considerable strength increase is induced by the presence of fibres, while in extension the strength increase is very limited. This is attributed to the fibre orientation distribution with respect to the tensile strains developed. Also presented in the paper is a framework for introducing the effects of fibres and their orientation into a constitutive model to describe the anisotropic stress-strain behaviour of fibre reinforced soils. Model simulations of selected test results are shown. Also described are examples of future investigations and trials required to make the soil reinforcement technology ready for use in industry.

1 INTRODUCTION

The growing demand for infrastructure, driven by increasing urbanization of populations, means that use of soil reinforcement and ground improvement technologies is rising by 10% annually. Reinforcement of soils by mixing with discrete flexible fibres is a relatively new technology with unique benefits that have not yet been widely exploited in industry. In very simple terms, fibre reinforcement gives a soil an ability to resist tensile strains. If used carefully, the technology may reduce lateral earth pressures acting on retention structures, aid the repair of unstable slopes, suppress the onset of liquefaction, and increase the ultimate bearing capacities and reduce settlements of shallow foundations.

Many laboratory studies have been conducted on fibre reinforced soils, typically involving direct shear tests, unconfined compression tests and conventional triaxial compression tests. The results clearly demonstrate that shear strength is increased and post-peak strength loss is reduced when discrete fibres are mixed with the soil (Al-Refeai, 1991; Maher and Ho, 1994; Yetimoglu and Salbas, 2003; Tang *et al.*, 2007; Diambra *et al*., 2007a, 2009). The effectiveness of the reinforcement is influenced by fibre type, volume fraction, length, aspect ratio, modulus of elasticity and also soil characteristics including particle size, shape and gradation, as well as stress level and density. It is not surprising that fibre orientation is particularly important (Jewell and Wroth, 1987; Palmeira and Milligan, 1989; Michałowski and Čermák, 2002 and Diambra *et al.*, 2009) and the most common procedure for preparing reinforced specimens in a laboratory, moist tamping, leads to preferred sub-horizontal orientation of fibres (Diambra *et al*., 2007b). A similar sub-horizontal orientation would result from using conventional earth moving and compaction equipment at field scale. Reinforced soils are more able to resist tension in directions aligned with heavy concentrations of fibres. Other laboratory studies show that fibre inclusions increase the number of cycles required to cause liquefaction during undrained loading (Noorany and Uzdavines, 1989; Maher and Woods, 1990). Also, static liquefaction of loose sands may be prevented by mixing with fibres (Ibraim *et al.*, 2009).

Most modelling approaches that have been proposed so far for fibre reinforced soil have focused on using just the concentration of fibres to explain shear strength increase (Gray and Ohashi, 1983; Jewell and Wroth, 1987; Maher and Gray, 1990; Ranjan *et al*., 1996; Michałowski and Zhao, 1996; Michałowski and Čermák, 2002, Michałowski, 2008 and Zornberg, 2002). There have been very few attempts to define a general constitutive model for reinforced soils (Ding and Hargrove, 2006; Li and Ding, 2002; Villard *et al.*, 1990; di Prisco and Nova, 1993). Only the models of Villard *et al.* (1990) and Diambra *et al.* (2007c, 2009) recognise the importance of fibre orientation in modelling fibre inclusions. Discrete element modelling has provided insight into the micromechanical aspects of the fibre/soil matrix interaction mechanism (Ibraim *et al.*, 2006; Ibraim and Maeda, 2007; Maeda and Ibraim, 2008) and may inform the development of ingredients for more conventionally used continuum models.

In this paper, results of drained and undrained triaxial test results are presented, as is a framework for introducing the effects of fibres and their orientation into a constitutive model for fibre reinforced soil. The model is used to simulate the test results with good success, and captures the anisotropic response.

2 NOTATIONS

Notations for axisymmetric triaxial conditions are adopted. p and q denote total mean and deviatoric stresses acting on the composite, respectively. The corresponding strain variables are the volumetric strain, ε_v, and shear strain, ε_q. These are related to axial and radial stresses and strains according to:

$$p = \frac{\sigma_a + 2\sigma_r}{3} \qquad q = \sigma_a - \sigma_r \qquad \varepsilon_v = \varepsilon_a + 2\varepsilon_r \qquad \varepsilon_q = \frac{2}{3}(\varepsilon_a - \varepsilon_r) \tag{1}$$

where subscripts a and r denote the axial and radial components respectively. The effective stress must be defined carefully. We use $p = p^* + u$, where p^* is the effective mean stress of the *composite* and u is the pore water pressure. The deviatoric stress of the *composite* will be denoted as q^*, even though it is unaffected by pore water pressure. The effective stress of the *composite* may be written in the abbreviated form $\boldsymbol{\sigma}^* = [p^*, q^*]^T$. This is related to the effective stress of the *soil matrix* $\boldsymbol{\sigma}' = [p', q']^T$ and the stress state of the *fibres* $\boldsymbol{\sigma}_f = [p_f, q_f]^T$ using the rule of mixtures:

$$\boldsymbol{\sigma}^* = v_m \boldsymbol{\sigma}' + v_f \boldsymbol{\sigma}_f \tag{2}$$

where v_m and v_f are volumetric concentration factors for the soil matrix and the fibres, respectively, defined as:

$$v_m = \frac{V_s + V_v}{V} = \frac{V - V_f}{V} \qquad v_f = \frac{V_f}{V} \qquad v_m + v_f = 1 \tag{3}$$

in which V, V_v, V_s and V_f are the volumes of the composite, voids, soil matrix and fibres, respectively. For an unreinforced soil, $v_f = 0$, $\boldsymbol{\sigma}_f = 0$, $v_m = 1$ and $\boldsymbol{\sigma}^* = \boldsymbol{\sigma}' = [p', q']^T$ represents the effective stress in the conventional way.

Equation 2 shows that the fibres and the soil matrix share the stresses applied to the composite. The concept of effective stress, a powerful tool used in the design of geotechnical infrastructure, needs to be carefully applied when using reinforced soils because when fibres act in tension they withstand load that would otherwise be taken by the soil matrix.

3 EXPERIMENTAL OBSERVATIONS

Hostun RF sand has been used in this study, as have Loksand™ flexible polypropylene crimped fibres. The fibres are of 35 mm length, are approximately circular in cross section with diameter of 0.1 mm, have a Young's modulus of 900 MPa and elastic limit of 200 MPa, and specific gravity of 0.91. Figure 1 shows fibres mixed into the sand.

The moist tamping technique used to prepare specimens has the advantage of a good control of specimen density while preventing the segregation of fibres and eventually produces a soil-fibre fabric which resembles that of compacted reinforced soils in the field. Cylindrical specimens with diameter 70 mm and height 70 mm were prepared in three layers of equal height to achieve target densities. The specimen diameter is twice the length of fibres and some localised non-uniformities and concentrations in the fibre distributions near the sample edges may have occurred. However, the effects of the sample boundary on the results have been assumed as negligible.

The average concentration of fibres included in a composite is defined as a percentage of dry weight of sand ($w_f = W_f/W_s$ x 100 (%), where W_f is the weight of fibres and W_s is the weight of the dry sand). A weight ratio is conveniently used for sample preparation purposes although the eventual modelling makes use of volume ratios (Equation 2). Nonetheless, the two ratios are directly related.

The void ratio must be carefully defined for a reinforced specimen, since the volume occupied by fibres can be "attached" either to the solid soil particles or to the voids. In this investigation the fibres have been considered as part of the solid.

3.1 FIBRE ORIENTATION DISTRIBUTION

When fibres are mixed into a soil and then compacted or tamped by applying energy through the vertical (x) axis, they will form an orientation distribution that is axially symmetric. The fibre orientations can be described by a general orientation distribution function $\rho(\theta)$ (Zhu *et al.*, 1994). $\rho(\theta)$ represents the volumetric concentration of fibres in an infinitesimal volume dV having an orientation of angle θ above the horizontal (yz) plane (Figure 2).

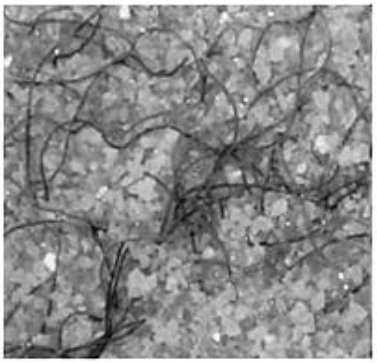

Figure 1: Polypropylene fibres mixed into sand.

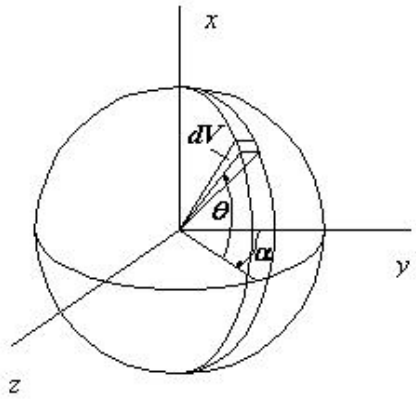

Figure 2: Coordinates used to define fibre orientation distribution function.

Diambra *et al.* (2007b) outlines a simple procedure for determining the fibre orientation distribution, which may be applied to laboratory specimens as well as reinforced soils prepared in the field, as long as there is an axial symmetry to the distribution. It involves cutting a reinforced soil along two orthogonal planes, where one plane is normal to the axis of symmetry and the other aligned with the axis of symmetry. The number of fibres intersecting finite areas on the two planes are counted, and used to fit the distribution function $\rho(\theta)$. For the reinforced sand specimens prepared using moist tamping considered here it was found that $\rho(\theta) = v_f \frac{2ab^2|\cos(\theta)|}{\cos(\theta)^2(b^2-a^2)+a^2}$, with a = 1.02 and b = 0.46, indicating that 97% of fibres are orientated with ±45° of the horizontal plane and 83% are orientated within ±30° of the horizontal plane.

3.2 DRAINED BEHAVIOUR

The results presented here were obtained using drained triaxial compression and extension tests conducted on fully saturated specimens. The isotropic consolidation pressure, $p^* = \sigma_r^*$, was 100 kPa. Lubricated ends were used at the top and bottom of the specimen. By visual inspection, the homogeneous shape of the specimen was well preserved at least up to 20% of axial strain in compression and -10% in extension.

Figures 3 and 4 present variations of q^* and ε_v with ε_a. The stress responses for unreinforced and reinforced specimens seem to be similar at low displacements suggesting that the initial stiffness of the sand-fibre composite is not influenced by the presence of fibres. With increasing axial strain and compressive loading the contribution of fibres to the strength of the composite increases and q^* for a reinforced specimen becomes greater than for an unreinforced one. An increase of the mobilised angle of friction by as much as 60% was recorded at 20% axial strain for loose specimens. Despite the fact that some compression tests were carried out until the axial strain reached 30 to 40%, the reinforced specimens show a linearly increasing stress-strain relationship that does not seem to flatten. This observation suggests that the interaction mechanism between the fibres and the sand matrix is not weakened by the deformation process, the fibres are not pulled out nor do they break. The reinforced sand is *failure resistant* for this type of loading and within the strain ranges considered which encompass those typical of geotechnical infrastructure. In triaxial extension the contribution of fibres to the deviatoric response appears to be very limited; the stress-strain relationships for reinforced specimens are almost identical to those for unreinforced specimens and the response is mostly controlled by the sand matrix. As mentioned earlier, the orientation of fibres in specimens prepared with a moist tamping technique are mostly closely aligned with the horizontal plane. As in a triaxial compression test the direction of the tensile strain is horizontal, the contribution of the fibres to the composite performance is enhanced by this particular orientation distribution. In a triaxial extension test most fibres are orientated in the direction of compressive strains and therefore have minimal influence on strength.

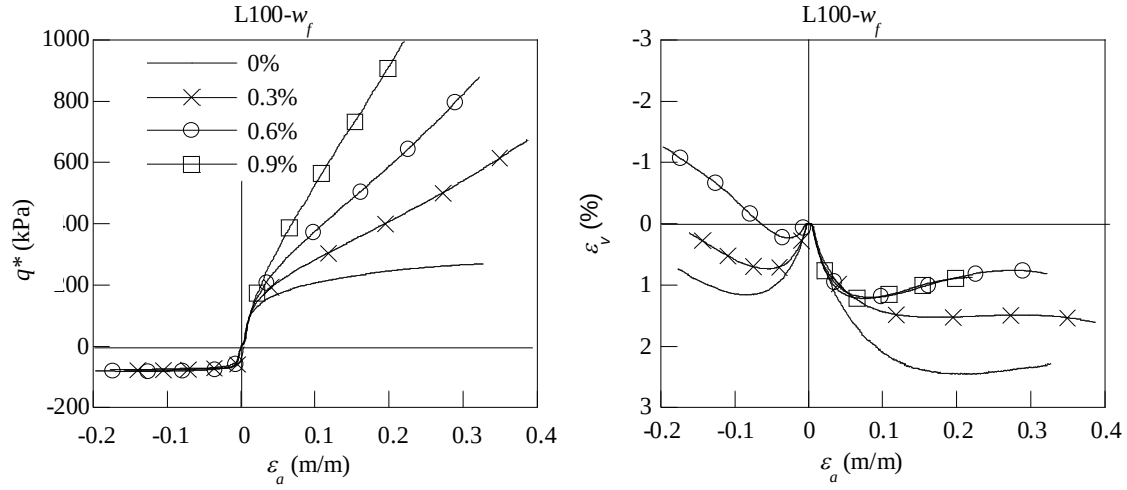

Figure 3: Triaxial test results for drained loose (L) specimens confined at 100 kPa cell pressure, with initial void ratios of 0.991, 0.966, 0.945 and 0.936 for 0%, 0.3%, 0.6% and 0.9% fibres by weight, respectively.

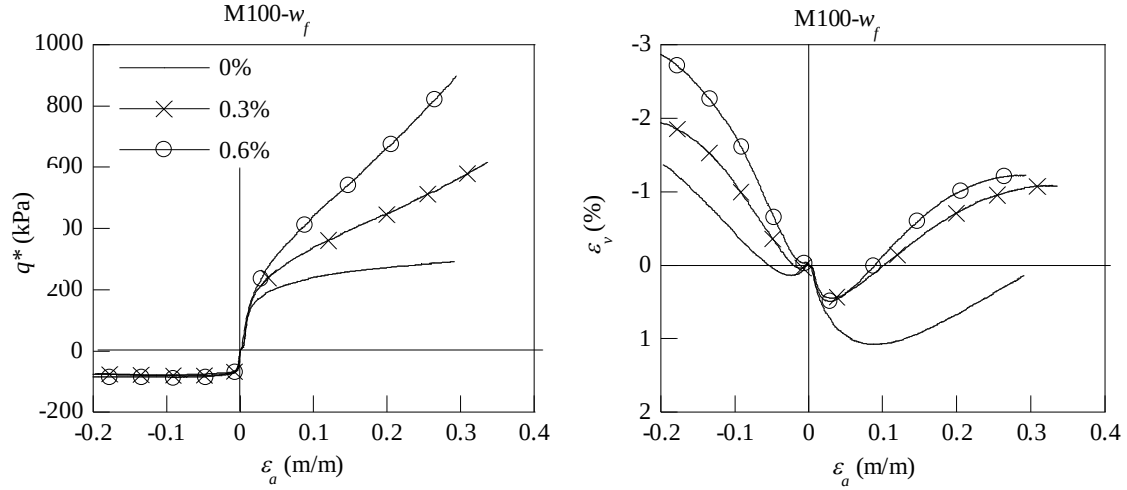

Figure 4: Triaxial test results for drained medium dense (M) specimens, confined at 100 kPa cell pressure, with initial void ratios of 0.914, 0.895 and 0.886 for 0%, 0.3% and 0.6% fibres by weight, respectively.

3.3 UNDRAINED BEHAVIOUR

Undrained triaxial compression and extension tests have been performed on loose reinforced sands, with isotropic consolidation pressures of 200 kPa. The results are presented in Figure 5.

Unreinforced specimens in compression, as well as in extension, show a progressive generation of pore pressure and continuous decrease of p^*. After a peak q^* is reached rapidly near the start of the test there is a sharp drop of q^* and stabilisation around a steady state as deformation continues. This is a characteristic of static liquefaction.

The presence of fibres strongly affects the undrained response and static liquefaction is fully prevented. In compression as well as in extension, the undrained stress paths of the reinforced specimens in the q^*:p^* plane initially follow closely the stress path of the unreinforced one. However, at certain points, the stress paths change direction sharply and show rapid changes in p^* and q^*. For a given confining pressure, these trajectories appear to have the same slope independent of fibre concentration. However, straight lines that best fit each trajectory, when extrapolated, do not intersect the origin of the q^*:p^* plane. The mobilised angle of friction ϕ_m^* of the reinforced specimens in compression increases monotonically with the shearing and, at 20% of shear strain, ranges from 44° to 52°. In extension, for all fibre

concentrations, the range of the mobilised angles of friction at 10% shear strain presents a narrow variation with values around 40±3°.

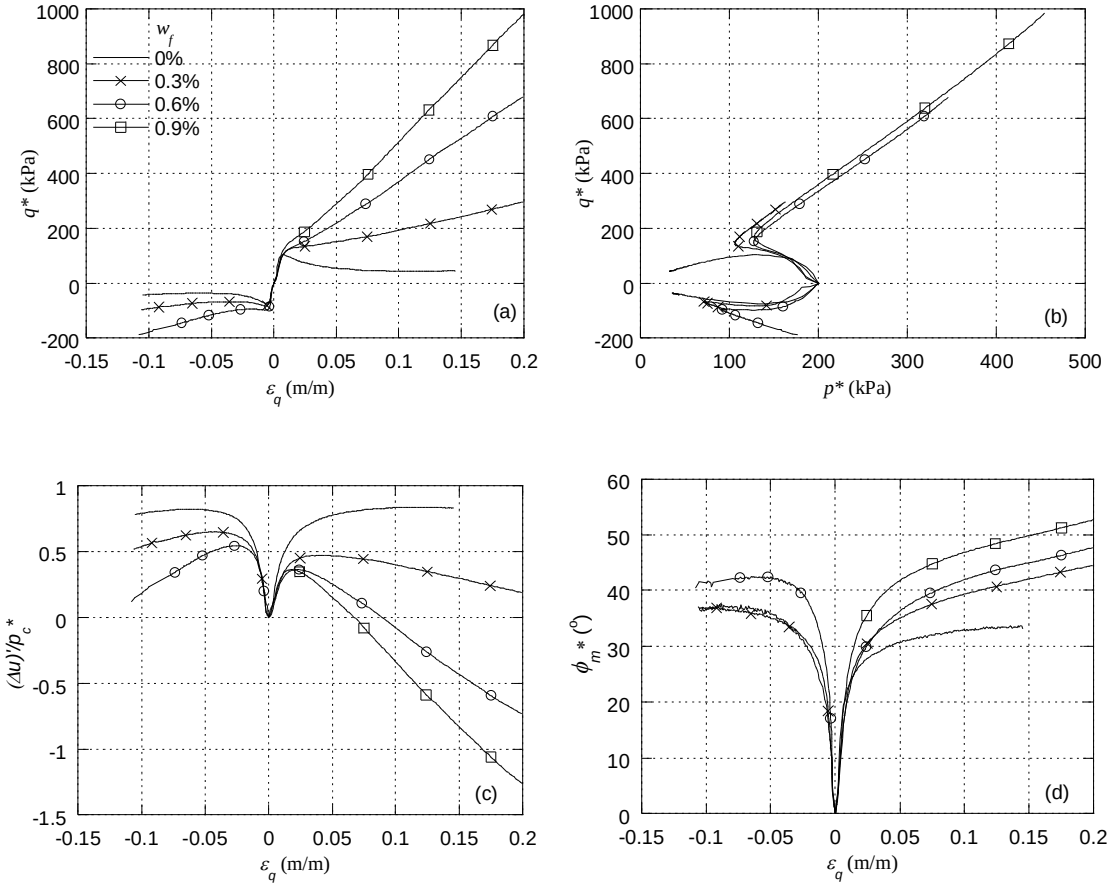

Figure 5: Undrained triaxial tests results for isotropic consolidation pressure of 200 kPa, with initial void ratios of 0.985, 0.963, 0.933 and 0.923 for 0%, 0.3%, 0.6% and 0.9% fibres (by weight), respectively.

4 CONSTITUTIVE MODELLING

4.1 FRAMEWORK

The rule of mixtures is used here for the development of a constitutive model for fibre reinforced soils. The sand matrix and fibres each satisfy their own constitutive laws, each is homogeneously distributed, and their individual contributions to the overall composite behaviour are made by scaling according to their volumetric fractions.

An expanded form of the incremental stress state of the composite is:

$$\dot{\boldsymbol{\sigma}} = \dot{\boldsymbol{\sigma}}' + v_f \dot{\boldsymbol{\sigma}}_f = [M_m]\dot{\boldsymbol{\varepsilon}} + v_f [M_f]\dot{\boldsymbol{\varepsilon}} \quad \textbf{(4)}$$

where M_m is the stiffness matrix for the soil component and M_f is the stiffness matrix for the fibres.

Equation 4 includes the minor simplifying assumption $v_m \approx 1$ which is reasonable since the volume of the fibres is very small compared to the volume of the composite. In Equation 4 Voigt's hypothesis is also assumed, meaning that the strain fields in the composite and the constituents are made equal. In other words, no sliding occurs between soil and fibres. However, an additional scale parameter may be introduced, as demonstrated later, to reduce the contribution fibres have on the composite if the no sliding assumption is removed.

The deformation of a single fibre embedded in the composite depends on its orientation. For conventional triaxial conditions, the incremental relationship between the strain at any angle θ from the horizontal ($\dot{\varepsilon}_\theta$) and the axial and radial strains is given by:

$$\dot{\varepsilon}_\theta = \dot{\varepsilon}_a \sin^2(\theta) + \dot{\varepsilon}_r \cos^2(\theta) \quad \textbf{(5)}$$

The stress carried by a fibre (behaving elastically with an elastic modulus E_f) oriented at an angle θ to the horizontal is then $\dot{\sigma}_{\theta f} = E_f \dot{\varepsilon}_\theta$ and it is possible to decompose this into equivalent stresses acting in the directions of the axial and radial stresses, $\dot{\sigma}_{af}(\theta)$ and $\dot{\sigma}_{rf}(\theta)$:

$$\dot{\sigma}_{af}(\theta) = \dot{\sigma}_{\theta f} \sin^2(\theta) \qquad \dot{\sigma}_{rf}(\theta) = \dot{\sigma}_{\theta f} \cos^2(\theta)/2 \quad \textbf{(6)}$$

In expanded form, Equation (6) can be rewritten as:

$$\dot{\sigma}_{af}(\theta) = E_f\left(\dot{\varepsilon}_a \sin^4(\theta) + \dot{\varepsilon}_r \cos^2(\theta)\sin^2(\theta)\right) \qquad \dot{\sigma}_{rf}(\theta) = E_f \frac{\left(\dot{\varepsilon}_a \sin^2(\theta)\cos^2(\theta) + \dot{\varepsilon}_r \cos^4(\theta)\right)}{2} \quad \textbf{(7)}$$

A non-uniform distribution of orientations is defined using the function $\rho(\theta)$. $\rho(\theta)$ represents the volumetric concentration of fibres in an infinitesimal volume dV having an orientation of angle θ above the horizontal plane (Figure 2). $\rho(\theta)$ also represents the volumetric concentration factor for the contribution of fibres within the composite with an orientation θ above the horizontal plane. The overall contribution of fibres within the composite in the directions of the axial and radial stresses (σ_{fa} and σ_{fr}) can then be obtained by integration over a representative composite volume using the following expressions:

$$\dot{\sigma}_{fa} = \frac{1}{V}\int_V \frac{\rho(\theta)}{v_f}\dot{\sigma}_{af}(\theta)\mathrm{d}V \qquad \dot{\sigma}_{fr} = \frac{1}{V}\int_V \frac{\rho(\theta)}{v_f}\dot{\sigma}_{rf}(\theta)\mathrm{d}V \quad \textbf{(8)}$$

For flexible fibres, only those fibres acting in tension contribute to the stresses of the composite. Therefore the integrations of Equation (8) should be performed within limits of θ for which $\dot{\varepsilon}_\theta < 0$. Defining $\theta_0 = \arctan\sqrt{-\dot{\varepsilon}_r/\dot{\varepsilon}_a}$ to be the direction of zero incremental strains (according to Mohr's circle for strain increment) then limits of the integration in (8) must correspond to $0 \le \theta \le \theta_0$ for triaxial compression and $\theta_0 \le \theta \le \pi/2$ for triaxial extension.

The bonding between fibres and soil may not be perfect and some amount of relative sliding between the two constituents may occur. An imperfect interfacial bond can be accounted for in the model with the introduction of a dimensionless sliding function f_b, which takes a value between 0 and 1. $f_b = 1$ for perfect bonding and $f_b = 0$ for full sliding. Introducing f_b means that the deformation of the fibres is not coincident with the deformation of the specimen which is instead given by $\dot{\boldsymbol{\varepsilon}}_f = f_b \dot{\boldsymbol{\varepsilon}}$. It follows that:

$$v_f\begin{bmatrix}\dot{\sigma}_{fa}\\ \dot{\sigma}_{fr}\end{bmatrix} = E_f f_b \begin{bmatrix} \int_{l_1}^{l_2}\rho(\theta)\cos(\theta)\sin^4(\theta)\mathrm{d}\theta & \int_{l_1}^{l_2}\rho(\theta)\cos^3(\theta)\sin^2(\theta)\mathrm{d}\theta \\ \frac{1}{2}\int_{l_1}^{l_2}\rho(\theta)\cos^3(\theta)\sin^2(\theta)\mathrm{d}\theta & \frac{1}{2}\int_{l_1}^{l_2}\rho(\theta)\cos^5(\theta)\mathrm{d}\theta \end{bmatrix}\begin{bmatrix}\dot{\varepsilon}_a\\ \dot{\varepsilon}_r\end{bmatrix} \quad \textbf{(9)}$$

where the integration limits are $l_1 = 0$ and $l_2 = \theta_0$ for compression loading and $l_1 = \theta_0$ and $l_2 = \pi/2$ for extension loading.

Returning to p and q triaxial notations, the contribution of fibres to the stresses in the composite can be expressed as:

$$v_f \dot{\boldsymbol{\sigma}}_f = E_f f_b [M_f]\begin{bmatrix}\dot{\varepsilon}_v\\ \dot{\varepsilon}_q\end{bmatrix} = E_f f_b \begin{bmatrix}A_{11} & A_{12}\\ A_{21} & A_{22}\end{bmatrix}\begin{bmatrix}\dot{\varepsilon}_v\\ \dot{\varepsilon}_q\end{bmatrix} \quad \textbf{(10)}$$

where:

$$A_{11} = \frac{1}{9}\left(F_{11} + F_{12} + 2F_{21} + 2F_{22}\right) \qquad A_{12} = \frac{1}{3}\left(F_{11} - \frac{F_{12}}{2} + 2F_{21} - F_{22}\right)$$

$$A_{21} = \frac{1}{3}\left(F_{11} + F_{12} - F_{21} - F_{22}\right) \qquad A_{22} = \frac{1}{2}\left(2F_{11} - F_{12} - 2F_{21} + F_{22}\right)$$

and the F_{ij} terms represent the components of the matrix of Equation (9) with the first subscript being the column number and the second subscript being the line number.

Any constitutive model for describing the stress-strain behaviour of the soil component of the composite may be used, such as the elastic-perfectly plastic Mohr-Coulomb model. In the elastic domain the increments of stresses are related to the increments of strains through the Young's modulus E and Poisson's ratio μ. Yielding occurs when the following relation is satisfied:

$$q' = Mp' \tag{11}$$

where M represents one of two properties M_c or M_e, depending on whether triaxial compression or triaxial extension is occurring, linked to the angle of friction ϕ' of the sand. When the soil yields the relationship between incremental plastic strains is controlled by:

$$\frac{\dot{\varepsilon}_v^p}{\dot{\varepsilon}_q^p} = -M^* \tag{12}$$

where M^* represents one of two properties M_c^* or M_e^*, depending on whether triaxial compression or triaxial extension is occurring, linked to the dilation angle of the sand.

4.2 SIMULATIONS

In simulating triaxial test results presented here the following input parameters were adopted: $\mu = 0.3$, $E = 40\,p_i^*$ (where p_i^* is the preconsolidation pressure), $\phi' = 34.5°$, a dilation angle that varies with density as per Bolton's (1986) relationship, and $E_f = 900$ MPa. The sliding function, f_b, which indirectly accounts for the imperfect interfacial bond between fibres and sand grains is one of the most difficult model ingredients to establish. A procedure based on a back analysis of the experimental results was used here to obtain $f_b = K_e\left(1 - \exp\left(-c_s\, p'/p_{ref}\right)\right)$ with $K_e = 0.6$, $c_s = 0.75$ and $p_{ref} = 100$kPa. The dependency of f_b on p' allows the simulation of an enhanced bonding between fibres and sand matrix at higher confining stresses as observed in the experiments.

Figures 6 and 7 compare model simulations with experimental results for conventional drained triaxial tests in the $q^* \sim \varepsilon_q$ and $\varepsilon_v \sim \varepsilon_q$ planes. The model simulations are represented by the thick continuous lines whereas the experimental data are represented with thin dotted lines. Despite the simplicity of the Mohr-Coulomb assumptions adopted for the sand matrix, the model generally reproduces the main features of the behaviour of unreinforced and reinforced specimens.

For compressive loading (Figure 6), the model captures well the somewhat bilinear nature of the reinforced soil response irrespective of fibre concentration, density and confining stress. The initial stress-strain responses generated by the model are not affected by the presence of fibres. In these initial parts the fibre contribution to the composite behaviour is quite small, which is not surprising as ε_r is also small, preventing the fibres from elongating and mobilising large tensile forces. At larger shear strains, the shear stress supported by the composite increases, apparently without limit, and this can be successfully reproduced by adopting a simple elastic model for the fibres and an anisotropic fibre orientation distribution. The presence of the fibres acts to increase the confinement of the sand matrix as the shear strain increases, allowing the sand to support greater deviatoric stresses. The assumption that the fibres are working within their elastic range seems correct for these fibres and these test conditions. In fact, careful examination of the fibres at the end of the triaxial tests showed no signs of fibre breakage or plastic deformation.

The limited contribution of fibres observed for extension loading is satisfactorily simulated by the model (Figure 7). In extension only very few fibres are orientated in the direction of tensile strains and this is taken into account by the fibre orientation distribution adopted.

The volumetric behaviour is, in general, well simulated. A correction has been introduced into the dilatancy relationship of the sand matrix to account for the occurrence of elastic strains in a reinforced specimen due to the extra confinement provided by fibres (details are given in Appendix 1 of Diambra *et al.*, 2009). The addition of fibres also affects the deformation behaviour of the assembly of sand grains, whose movements are influenced by the physical presence of fibres. In the extension tests, the volumetric behaviour is not simulated as well as that for the compression tests because

the initial plastic volumetric strains have opposite magnitude to elastic volumetric strains and this cannot be reproduced adopting a simple Mohr-Coulomb model. The use of more complex models for the soil matrix will enable improved fits between simulations and experiment.

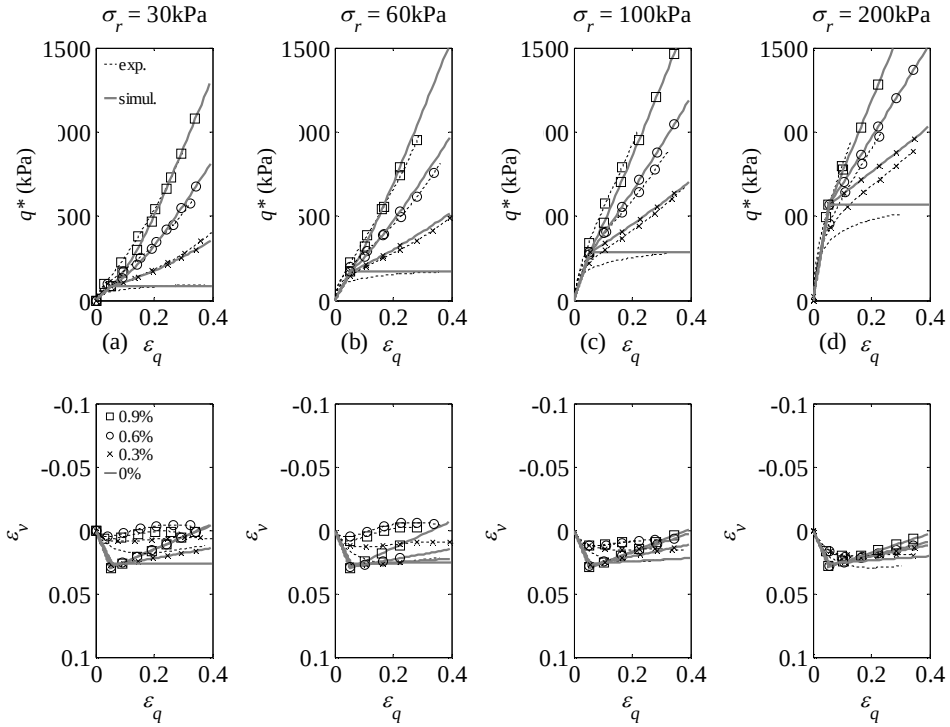

Figure 6: Triaxial compression test results and model simulations for reinforced and unreinforced specimens.

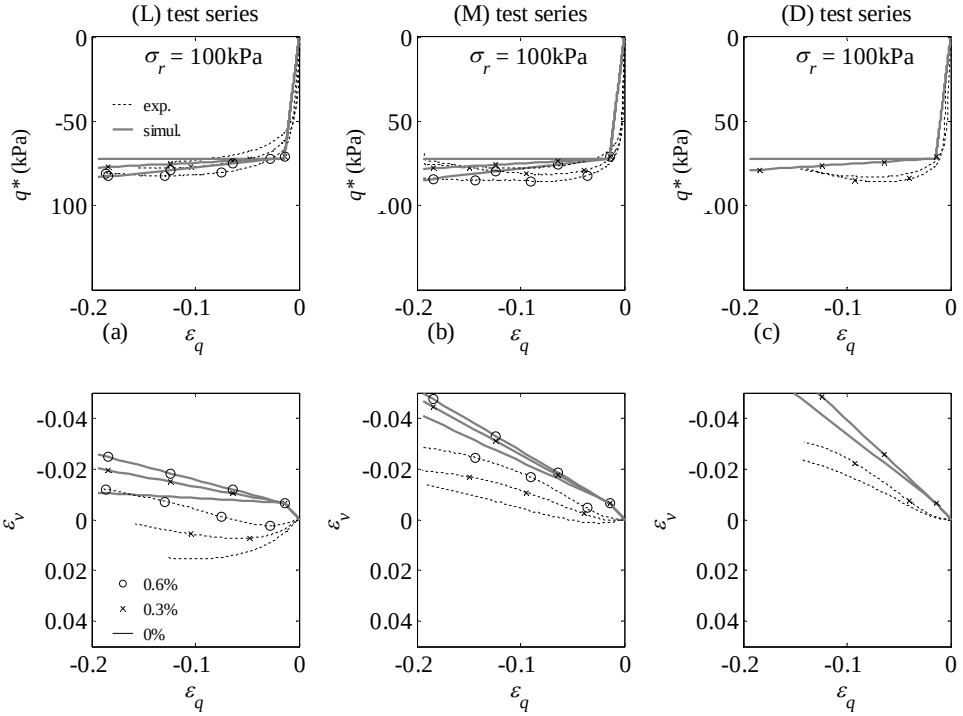

Figure 7: Triaxial extension test results and model simulations for loose (L), medium dense (M) and dense (D) reinforced and unreinforced specimens.

5 CONCLUSIONS AND FUTURE WORK

Drained and undrained triaxial test results highlight how soil stress-strain behaviour may be altered by mixing with discrete flexible fibres. In triaxial compression a considerable increase of strength is created by the presence of fibres, while in extension the benefit of fibres is very limited. Most research on fibre reinforced soils up until now has been concerned only with the compressive triaxial behaviour. The conclusions of those studies which show large strength increases must be applied carefully as the fibre reinforced soil composite shows a definite anisotropy. Assuming a random orientation of fibres would be inappropriate and lead to non conservative misrepresentations in estimated strength increases.

A simple modelling approach for fibre reinforced soil has been presented, based on the rule of mixtures. Model simulations exhibit key features that were also observed in triaxial test results. Discrepancies between simulation and experimental results can be attributed to the simplistic nature of the Mohr-Coulomb model used for the soil component - a closer fit between simulation and experiment would be obtained by adopting a more complex model that captures soil non-linearity. The modelling approach permits the use of any fibre orientation distribution function. It also accounts for the evolution of fibre orientation as the composite deforms.

There is potential for massive cost savings and improvements in strength and safety of geotechnical infrastructure when fibre reinforced soils are used. There is a need for physical and numerical model tests to further understand this technology, to further validate the constitutive framework for a range of reinforced soil types, and to provide recommendations for application in a safe and reliable way.

Physical model tests, performed in a laboratory controlled environment with appropriate instrumentation and monitoring, may include plate bearing tests and strip load tests, which resemble loading conditions around shallow footings. Tests involving variations in lateral earth pressure may also be used to simulate conditions in soil supported by a retaining wall. Centrifuge testing may be used to investigate potential applications in slope stabilisation. Shaking table and shear stack tests may be used to investigate dynamic behaviour and liquefaction potential. Physical model tests may also involve field prototypes, for example in sections of pavements where base course and subgrade materials have been reinforced. There is also a need to trial a range of field mixing procedures, whether they involve mechanical mixing and placement/compaction or hydraulic mixing and deposition.

Numerical analyses of the physical model tests should be conducted involving appropriate constitutive equations for reinforced soil behaviour accounting for fibre orientation. The analyses will demonstrate whether or not the constitutive laws governing reinforced soil behaviour in triaxial tests also govern behaviour when subjected to loading conditions more similar to real geotechnical engineering problems.

Design tools may be developed following physical model tests and supporting numerical analyses. Accurate cost-benefit assessments may then be possible.

6 REFERENCES

Al Refeai, T.O., 1991. Behaviour of granular soils reinforced with discrete randomly oriented inclusions. *Geotextiles and Geomembranes*, 10, 319-333.

Bolton, M.D., 1986. The strength and dilatancy of sands. *Géotechnique*, 36(1), 65-78.

Boominathan, A, Hari, S., 2002. Liquefaction strength of fly ash reinforced with randomly distributed fibres. *Soil Dynamics and Earthquake Engineering*, 22, 1027-1033.

di Prisco, C., Nova, R., 1993. A constitutive model for soil reinforced by continuous threads. *Geotexiles and Geomembranes*, 12,161-178.

Diambra, A., Ibraim, E., Russell, A.R., Muir Wood, D., 2007a. Shear tests on fibre reinforced sands. *Proceedings of 5th International Symposium on Earth Reinforcement*, (Taylor&Francis Ed.) Balkema, 329-334.

Diambra, A., Russell, A.R., Ibraim, E., Muir Wood, D., 2007b. Determination of fibre orientation distribution in reinforced sand. *Géotechnique*, 57(7), 623-628.

Diambra, A., Russell, A.R, Ibraim, E.,., Muir Wood, D., 2007c. Modelling fibre reinforced sands. *Proceedings of 5th International Symposium on Earth Reinforcement*, (Taylor&Francis ed.) Balkema, 379-385.

Diambra, A., Ibraim, E., Muir Wood, D., Russell, A.R., 2009. Fibre Reinforced Sands: Experiments and Modelling. *Geotextiles and Geomembranes* (accepted for publication).

Ding, D., Hargrove, S.K., 2006. Nonlinear stress-strain relationship of soil reinforced with flexible geofibers. *Journal of Geotechnical & Geoenvironmental. Engineering, ASCE* 132(6),791-794.

Gray, D.H., Ohashi, H., 1983. Mechanics of fiber reinforcement in sands. *Journal of Geotechnical Engineering, ASCE* 109(3), 335-353.

Ibraim, E., Muir Wood, D., Maeda, K., Hirabashi, H., 2006. Fibre-reinforced granular soils behaviour. *International Symposium on Geotechnics of Particulate Media*, Yamaguchi, Japan, 443-448.

Ibraim, E., Maeda, K., 2007 Numerical analysis of fibre-reinforced granular soils. *Proceedings of 5th International Symposium on Earth Reinforcement*, (Taylor&Francis ed.) Balkema,387-393.

Ibraim, E., Diambra, A., Muir Wood, D. and Russell, A.R. 2009. Static liquefaction of fibre reinforced sand. *Geotextiles and Geomembranes* (submitted for possible publication).

Jewell, R.A., Wroth, C.P., 1987. Direct shear tests on reinforced sand. *Géotechnique* 37 (1), 53-68.

Li, J., Ding, D.W., 2002. Nonlinear elastic behavior of fiber-reinforced soil under cyclic loading. *Soil Dynamics and Earthquake Engineering*, 22, 977–983.

Maeda, K. & Ibraim, E., 2008. DEM analysis of 2D fibre-reinforced granular soils. *Proceedings of 4th Int. Symp. on Deformation Characteristics of Geomaterials*, Atlanta, USA, 623-628.

Maher, M. H., Woods, R. D. 1994. Dynamic response of sands reinforced with randomly distributed fibers. *Journal of Geotechnical Engineering Division, ASCE*, 116 (7), 1116-1131.

Maher, M.H., Gray, D.H., 1990. Static response of sand reinforced with fibres. *Journal of Geotechnical Engineering, ASCE* 116(11), 1661-1677.

Maher, M.H., Ho, Y.C., 1994. Mechanical properties of kaolinite/fiber soil composite. *Journal of Geotechnical Engineering Division, ASCE* 120 (8), 1381–1393.

Michałowski, R.L., 2008. Limit analysis with anisotropic fibre-reinforced soil. *Géotechnique*, 58(6), 489-501.

Michałowski, R.L., Čermák, J., 2002. Strength anisotropy of fiber-reinforced sand. *Computers and Geotechnics*, 29, 279-299.

Michałowski, R.L., Zhao, A., 1996. Failure of fiber-reinforced granular soils. *Journal of Geotechnical Engineering, ASCE* 122(3), 226-234.

Noorany, I., Uzdavines, M. 1989. Dynamic behavior of saturated sand reinforced with geosynthetic fabrics. *Proc., Geosynthetics '89 Conf.*, Vol. II, San Diego, California, 385-396.

Palmeira, E.M., Milligan, G.W.E., 1989. Large scale direct shear tests on reinforced soil. *Soils and Foundations*, 29(1), 18-30.

Ranjan, G., Vasan, R.M., Charan, H.D., 1996. Probabilistic analysis of randomly distributed fiber-reinforced soil, *Journal of Geotechnical Engineering, ASCE* 122(6), 419-426.

Tang , C., Shi, B., Gao, W., Chen,F., Cai,Y., 2007. Strength and mechanical behaviour of short polypropylene fiber reinforced and cement stabilized clayey soil. *Geotexiles and Geomembranes*, 25, 194-202.

Villard, P., Jouve, P., Riou, Y., 1990. Modélisation du compertment mécanique du Texsol. Bulletin liaison Labo. P et Ch. 168, 15-27.

Yetimoglu, T., Salbas, M., 2003. A study on the shear strength of sands reinforced with randomly distributed discrete fibres. *Geotexiles and Geomembranes*, 21, 103-110.

Zhu, Y.T., Zong, G., Manthiram, A., Eliezer, Z., 1994 Strength analysis of random short-fibre-reinforced metal matrix composite materials. *Journal of Material Science*, 29, 6281-6286.

Zornberg, J.G., 2002 Discrete framework for equilibrium analysis of fibre-reinforced soil. *Géotechnique*, 52(8), 593-604.